The IPHAS-POSS-I proper motion survey of the Galactic plane

N. R. Deacon,[1]⋆ P. J. Groot,[1] J. E. Drew,[2] R. Greimel,[3,4] N. C. Hambly,[5] M. J. Irwin,[6] A. Aungwerojwit,[7,8] J. Drake[9] and D. Steeghs[8,9]

[1]*Department of Astrophysics, IMAPP, Radboud University Nijmegen, PO Box 9010, 6500 GL Nijmegen, the Netherlands*
[2]*Centre for Astrophysics Research, University of Hertfordshire, College Lane, Hatfield AL10 9AB*
[3]*Isaac Newton Group of Telescopes, Apartado de correos 321, E38700 Santa Cruz de La Palma, Tenerife, Spain*
[4]*Institut für Physik, Karl-Franzen Universität Graz, Universitätsplatz 5, 8010 Graz, Austria*
[5]*SUPA†, Institute for Astronomy, School of Physics, University of Edinburgh, Royal Observatory Edinburgh, Blackford Hill, Edinburgh EH9 3HJ*
[6]*Institute of Astronomy, Madingley Road, Cambridge CB3 0HA*
[7]*Department of Physics, Faculty of Science, Naresuan University, Phitsanulok 65000, Thailand*
[8]*Department of Physics, University of Warwick, Coventry CV4 7AL*
[9]*Harvard-Smithsonian Center for Astrophysics, Cambridge MA 02138, USA*

ABSTRACT

We present a proper motion survey of the Galactic plane, using Isaac Newton Telescope (INT) Photometric Hα Survey (IPHAS) data and Palomar Sky Survey (POSS)-I Schmidt plate data as a first epoch, that probes down to proper motions below 50 mas yr^{-1}. The IPHAS survey covers the northern plane ($|b| < 5°$) with CCD photometry in the r, i and Hα passbands. We examine roughly 1400 deg^2 of the IPHAS survey area and draw up a catalogue containing 103 058 objects with significant proper motions below 150 mas yr^{-1} in the magnitude range $13.5 < r' < 19$. Our survey sample contains large samples of white dwarfs and subdwarfs which can be identified using a reduced proper motion diagram. We also found several objects with IPHAS colours suggesting Hα emission and significant proper motions. One is the known cataclysmic variable GD552; two are known DB white dwarfs and five others are found to be non-DA (DB and DC) white dwarfs, which were included in the Hα emission line catalogue due to their lack of absorption in the Hα narrow band.

Key words: surveys – astrometry.

1 INTRODUCTION

The INT Photometric Hα Survey (IPHAS; Drew et al. 2005) is a deep ($r < 21$), CCD based survey in three filters ($r, i,$ Hα) covering 1800 deg^2 of the northern Galactic plane ($|b| < 5°$). IPHAS forms part of the European Galactic Plane Surveys (EGAPS), which also includes the United Kingdom Infrared Telescope Infrared Deep Sky Survey Galactic Plane Survey (Lawrence et al. 2007; Lucas et al. 2008) covering 1800 deg^2 of the plane in J, H, K to a depth of $K = 19$ and the UV (ultraviolet) EXcess survey (UVEX; Groot et al. 2009). UVEX is planned to complement IPHAS by covering the same area but in u, g and He I 5875 Å with an additional r-band epoch. These surveys also have upcoming southern counterparts. With the number density of stars highly concentrated on the plane, IPHAS and EGAPS provide ideal tools to study a whole range of stellar and Galactic research topics. They have already yielded sig-

nificant discoveries in fields such as cataclysmic variables (Witham et al. 2008), planetary nebulae (Mampaso et al. 2006; Wesson et al. 2008), young low-mass objects (Valdivielso et al. 2009), star-forming regions (Vink et al. 2008) and extinction in the Galactic plane (Sale, Drew & Unruh 2009). Large-scale CCD-based astronomical surveys such as IPHAS provide accurate photometric and astrometric data on large numbers of astronomical objects. In addition to their main science goals, surveys such as EGAPS make their data public (see Gonzalez-Solares et al. 2008 for details on public IPHAS data) and they can be used by anyone in the astronomical community to pursue their own research aims. Combining IPHAS data with those from other surveys with different wavebands or epochs can lead to discoveries of variable objects and can also allow the parameter space of each object to be expanded to include not only magnitudes and positions but proper motions as well. Here, we undertake the first comprehensive, optical, wide-field survey to identify proper motions below 0.1 arcsec yr^{-1} in the Galactic plane by cross-referencing the IPHAS data base with SuperCOSMOS (Hambly et al. 2001) scans of the POSS-I plates taken in the 1950s. This gives us a proper motion baseline of approximately 50 years.

⋆E-mail: ndeacon@astro.ru.nl
†Scottish Universities' Physics Alliance

Early proper motion surveys utilized blink comparators and exceptional patience to indentify moving stars manually. The early manual work of Luyten is brought together in two samples, the Luyten Half-Arcsecond Survey (Luyten 1979a) which catalogued 3561 objects with proper motions greater than half an arcsec per year and the New Luyten Two Tenths Catalogue (NLTT, Luyten 1979b) which contained 58 845 objects with $\mu > 0.2$ arcsec yr^{-1}. Both these surveys ran into difficulties in the Galactic plane with the NLTT survey less than 50 per cent complete for $|b| < 15°$ at magnitudes fainter than $V = 16$ (Lepine & Shara 2005). The main modern computational study is that of Lepine (2008). They used a sophisticated algorithm to degrade POSS-II images to the same quality as the older POSS-I images. The two could then be subtracted and high proper motion stars identified. This survey is complete to $V = 20$ and $\mu = 0.15$ arcsec yr^{-1}. However, the survey suffers from crowding in the Galactic plane leading to a reduction in completeness. Lepine & Shara estimate they are only 80–90 per cent complete down to $V = 19$ within $15°$ of the Galactic plane. Fedorov, Myznikov & Akhmetov (2009) predict their upcoming catalogue will cover low proper motions in the Galactic plane but will not provide a consistent proper motion range due to a varying maximum proper motion. Gould & Kollmeier (2004) used data from the Sloan Digital Sky Survey photographic plate data to produce a proper motion survey below 100 mas yr^{-1}. However, this avoided the Galactic plane. The study of Folkes et al. (2007) attempts to fill in the Galactic plane gap left by southern surveys such as Deacon & Hambly (2007), Pokorny et al. 2003 and Finch et al. (2007) (all of which avoid the plane) by combining United Kingdom Schmidt Telescope (UKST) and Two-Micron All-Sky Survey (2MASS) data in a similar manner to Deacon & Hambly (2007) to identify candidate low-mass stars and brown dwarfs from their proper motion.

2 METHOD

In order to plan our proper motion survey, we had to first consider the data sets available. Two data sets are available for use as a first epoch, both having been scanned using the SUPERCOSMOS plate scanning machine (Hambly et al. 2001). Also as well as the POSS-I plates, the newer, higher quality POSS-II plates with better emulsion sensitivity and improved resolution are available. These provide better astrometric accuracy but a much shorter time baseline with respect to IPHAS (10–15 years compared to the IPHAS data versus the roughly 50 yr epoch difference betweeen IPHAS and POSS-I). However, a shorter baseline means less contamination due to spurious pairings; $n_{\text{spurious}} \propto (\mu_{\text{max}} \Delta t)^2$, where n_{spurious} is the number of spurious pairings, μ_{max} is the maximum proper motion and Δt is the epoch difference. n_{spurious} is also proportional to the density of objects around the target. This is one of the reasons most proper motion surveys have avoided higher density areas of the sky such as the Galactic plane.

Along with these data, we also have the upcoming UVEX survey (Groot et al. 2009) which will be a blue companion to IPHAS and a second r epoch. This will provide us with CCD quality second epoch astrometry, observed by the same telescope and camera, reduced by the same pipeline but with only a 3–5 yr baseline. Examining the positional errors between IPHAS and UVEX, we found that they were typically 40 mas (see Fig. 1), rising to 50 mas at $r = 19$ (where POSS-I plate astrometry becomes difficult; see Fig. 2) and to roughly 100 mas, as the survey limit ($r \sim 21$) is approached. Hence, we can assume that with a 3 yr baseline, the minimum 5σ proper motion detectable between IPHAS and UVEX
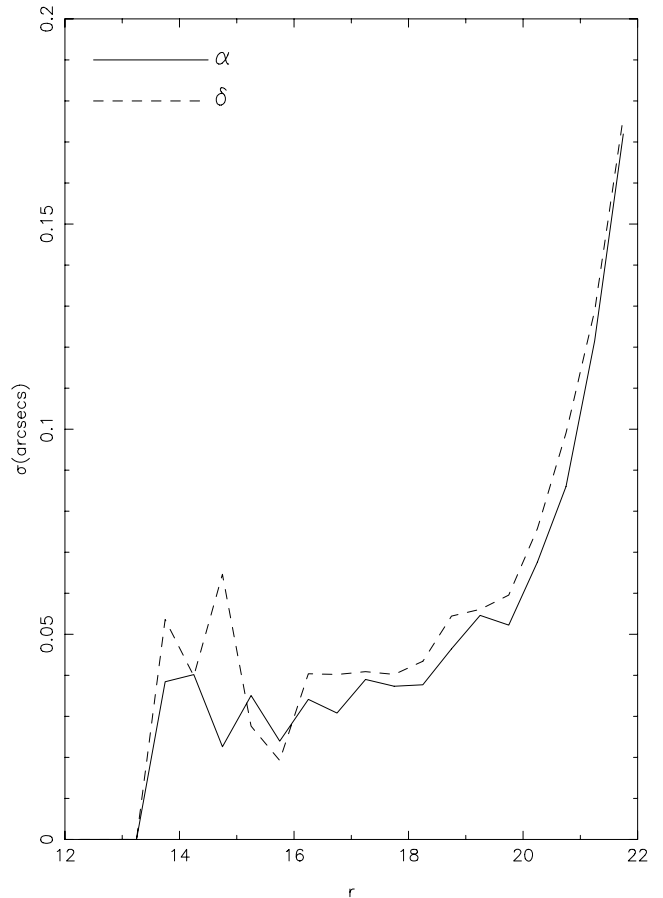

Figure 1. The astrometric errors (in arcsec) between the IPHAS and UVEX surveys.

at the survey limit ($r \sim 21$) is roughly 166 mas yr^{-1}. At the limit at which astrometry on the POSS-I plates becomes difficult ($R_F = 19$), the minimum proper motion becomes 100 mas yr^{-1}. Hence, below this latter limit (also below the $\mu = 0.15$ mas yr^{-1}, lower proper motion limit of Lepine & Shara 2005 and Lepine 2008) there is the potential for a lower proper motion survey to probe to previously unexplored proper motions in the Galactic plane. To coincide with the lower limit of a potential IPHAS–UVEX proper motion survey (less than 100 mas yr^{-1} for objects brighter the $r = 19$) and leaving some overlap, we decided on a maximum proper motion of 0.15 arcsec yr^{-1}. This means that even with the exceptionally long baseline between IPHAS and the POSS-I plates the maximum pairing radius is only $\sim$10 arcsec, making spurious pairings unlikely. This is due not only to the low chance probability of another object lying in this region near to the target but also because many chance objects which lie so close to the target may also be deblended by the SUPERCOSMOS software Hambly et al. (2001). For reasons of poor astrometry, we have excluded all deblended objects. The advantage of the POSS-II plates over the POSS-I plates is their better astrometry and photometry. However with the long IPHAS-POSS-I time baseline, even this better quality POSS-II astrometry cannot produce a lower minimum proper motion than using POSS-I plates and we have CCD quality photometry available from the IPHAS survey. The SUPERCOSMOS scans of POSS-I plates only extend to $\delta \sim 2°5$, south of this we use SUPERCOMSOS UK Schmidt Telescope R plates.

Before beginning the proper motion survey, it is important to have both surveys on the same astrometric framework as our initial
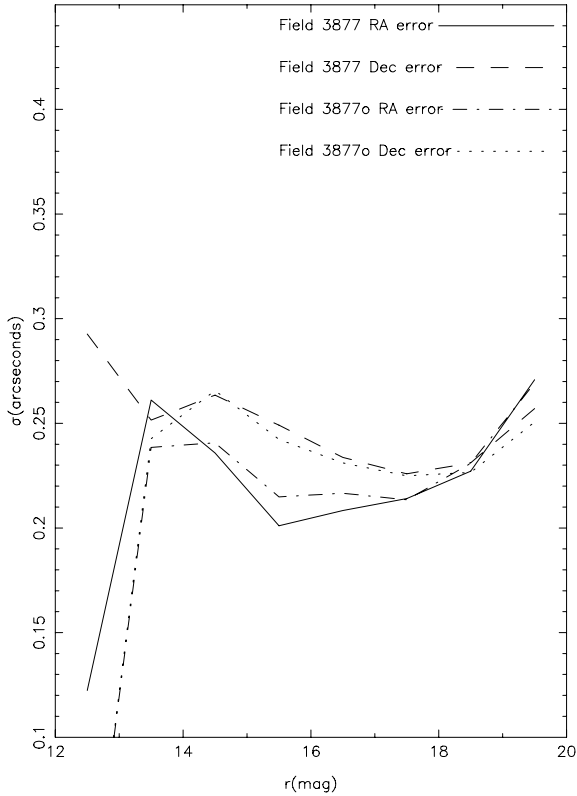
Figure 2. The astrometric errors (in arcsec) between the IPHAS and POSS-I data.

calculations will be based on the global astrometric frameworks of both surveys. IPHAS is tied to the 2MASS astrometric framework so we converted the POSS-I astrometry to the 2MASS astrometric reference frame. This was done in an identical way to the transformation of UKST *I* plates to the 2MASS system described in section 2.1 of Deacon & Hambly (2007).

In order to estimate the minimum significant positional shift that can be detected, we robustly calculated the positional errors between the POSS-I plates and the IPHAS survey (the error estimates calculated between the IPHAS and UVEX surveys found in Fig. 1 were calculated in the same way). This was done by identifying the same objects in each epoch and calculating the positional differences. These were then binned by magnitude and the error calculated (Fig. 2). After examining this plot, we determined the 5σ positional shift to be at 1 arcsec, this was then used as our minimum positional shift. This means our minimum proper motion will be roughly 20 mas yr^{-1}. As we will calculate relative astrometric solutions for each object in our final catalogue, this number may vary slightly.

Our search methodology was as follows. Objects which were flagged as stellar sources or probable stellar sources (classification flags −1 and −2; Drew et al. 2005) in IPHAS were selected. This excludes saturated sources and hence introduces a bright limit to our survey at approximately $r = 13.5$. One initial problem encountered was the difference in the sizes of the point spread functions (PSF) of the two surveys. Often two stars with a small separation which are resolved in IPHAS will be blended together on the lower-resolution POSS plates leading to the erroneous conclusion that one or both of them have moved. To remove this potential source of contamination, any IPHAS object of brightness $r = x$ (where x is in magnitudes) which had another IPHAS object brighter than $x − 2$ within 6 arcsec was excluded. This magnitude difference was selected as typically

objects which are 2 or more magnitudes fainter than an object will not significantly affect its astrometry. This pairing radius increased at brighter magnitudes, in line with the rough size of the POSS-I PSF (up to 20 arcsec for stars brighter than $r = 9$).

Subsequently, IPHAS objects which were not affected by such crowding had their positions compared with the POSS-I data to see if they had a companion within an arcsecond. If they did, they were judged not to have a significant proper motion and hence were excluded. Any potential POSS-I pair for these unpaired objects was then searched for. First, the region within 6 arcsec was searched and if no pair was found the region within $r_{max} = \mu_{max}\Delta t$ was searched. Any potential pair had to have a POSS-I R_F magnitude within 3σ (where σ is approximated from the values for measurement errors quoted in Hambly et al. 2001, roughly 0.2 mag at best[1]) of the IPHAS r magnitude and had to be stellar sources which had not been deblended and were not in close proximity to bright stars (note this 3σ cut could exclude high proper motion variables). To ensure that the paired POSS-I object does not have an IPHAS counterpart, the POSS-I positions were cross-checked with IPHAS positions and any object with an IPHAS pair within 1 arcsec was excluded.

2.1 Calculation of astrometric solution

In order to gain an insight into the local astrometric accuracy of each proper motion measurement, a local relative astrometry mapping was carried out for each candidate. To do this, all objects in the same IPHAS field as the target with brightnesses within 1 mag of the star in question were selected. These were then used to produce a six-parameter plate–plate fit using SLALIB routines (Wallace 1998) to determine the astrometric differences between the two reference frames and to estimate the random errors remaining once these differences have been corrected for. This fit was then applied and used to calculate a proper motion relative to this reference frame. This also yielded measures of the positional errors for each field. However, in cases with few reference stars (i.e. <20) the error will be underestimated. To correct for this, we carried out a series of simulations. Sets of reference stars on two different reference frames were created. These were given small random bulk offsets between the reference frames and individual random Gaussian errors. A fit between the reference frames was carried out and the calculated positional error compared to the individual positional errors used. It was found that for few reference stars the error was underestimated. We find that the correction factor is well fitted by the equation,

$$\frac{\sigma_{true}}{\sigma_{measured}} \approx 1 + \frac{19.8}{n_{ref}^{1.5}}, \qquad (1)$$

where σ_{true} is the actual error, $\sigma_{measured}$ the measured error and n_{ref} the number of reference stars. We find this relation holds fairly well down to as few as six reference stars. This correction factor was used to ensure all our quoted errors are accurate. Where there were not enough reference stars for any fit, an error calculated from the global positional error estimates shown in Fig. 2 was used.

3 RESULTS

The final catalogue consists of 103 058 objects spread across 14 126 IPHAS fields (including overlap fields) where the area of each field is roughly 0.3 deg^2. These objects all have proper motions more

---

[1] Note as the IPHAS photometric errors are typically much smaller than POSS-I errors we ignore them in our error estimation.
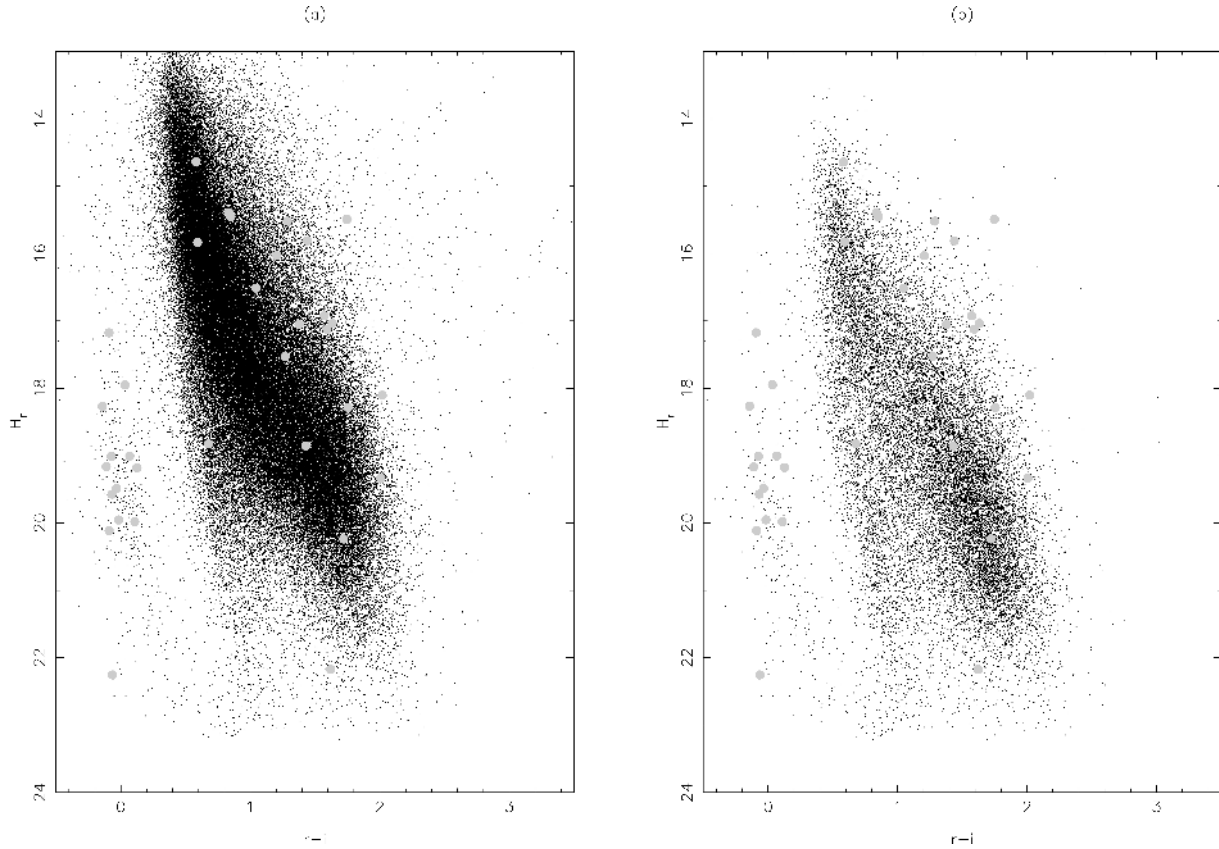
Figure 3. Two reduced proper motion diagrams for our data set. Panel (a) shows all objects in our sample and panel (b) shows only those with μ greater than 50 mas yr^{-1}. The populations shown are as follows: the main locus is the main sequence, below and to the left are the higher velocity and bluer subdwarfs and to the left of them are the intrinsically fainter white dwarfs. The large grey dots represent the objects common between this catalogue and the catalogue of H$_\alpha$ emitters from Witham et al. (2008). These are all plotted on both panels, regardless of their proper motions.

significant than 5σ where the proper motion errors were typically below 10 mas yr^{-1} (i.e. $\mu_{min} < 40$ mas). A full list of all these objects will be provided in the online version of the paper (see Supporting Information). To check the sample, a reduced proper motion diagram (Luyten 1922, credited to Hertzprung) was produced. Reduced proper motion takes observables (proper motion and apparent magnitude) and combines them in such a way that the result only depends on characteristics of the star (tangential velocity and absolute magnitude). The definition we use is given below,

$$H_r = r + 5 \log_{10} \mu + 5 \log_{10}(47.4)$$

$$H_r = M_r + 5 \log_{10} d - 5 + 5 \log_{10} v_T - 5 \log_{10}(4.74)$$
$$- 5 \log_{10} d + 8.379$$

$$H_r = M_r + 5 \log_{10} v_T, \tag{2}$$

where μ is the proper motion in arcsec yr^{-1}, d is the distance in parsecs and v_T is the tangential velocity in km s^{-1}. The above definition of reduced proper motion is not the most commonly used but is useful as it removes the constants needed to convert between units. Our reduced proper motion diagram is shown in Fig. 3. The form is roughly what we would expect from a standard Galactic stellar population with clearly identifiable dwarf, subdwarf and white dwarf loci. However, after we studied the spatial distribution of objects it was found that there were several fields with many (more than 250) objects. After some investigation, it became clear that these fields had poor astrometric solutions in the IPHAS data (mostly due to poor observing conditions). When we examined a

histogram of number of detected objects per field, it was found that these fields lay beyond the point where the main distribution had died away. Additionally, when the reduced proper motion diagrams for objects in these fields were examined it was found that it did not contain the expected population distributions, indicating that the proper motion determinations were not correct. Hence, any object lying in these fields was excluded from the final catalogue. A plot of the spatial distribution of the remaining objects can be found in Fig. 4. It shows that for the majority of the northern plane the coverage is good with a few patches of incompleteness. However, moving along the plane towards the Galactic Centre the number of objects drops off dramatically. This is due to our selection criteria excluding crowded regions as well as large numbers of objects in these regions being blended with other images (again a result of high stellar density). This can be seen in Fig. 5 which shows the density of stellar sources in each IPHAS field: there are clearly fewer high proper motion objects detected in areas of higher stellar density.[2] This is also shown by the inverse correlation between the density of stellar sources in a field and the typical number of detected proper motion sources in that field (see Fig. 6). Fig. 7 shows an IPHAS colour–colour plot for our objects. The main locus is a clear, unreddened main sequence (see Drew et al. 2005), widened by the fact that the IPHAS photometry is not yet globally calibrated. Approximately, 96 per cent of objects in the catalogue lie on or close to

---

[2] The general trend towards more crowded fields towards the Galactic Centre can be seen in fig. 3 of Gonzalez-Solares et al. (2008).
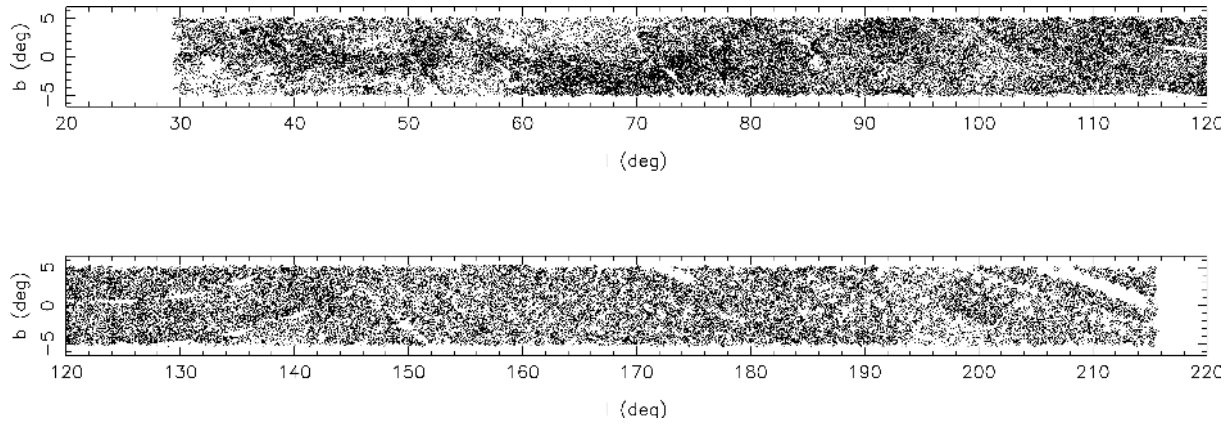
Figure 4. Distribution of objects in our sample across the Galactic plane. The coverage is in general good; however, the coverage appears patchy in parts, particularly at low Galactic longitude ($l < 90$). Also note the areas with no coverage, these either lie outside the survey area (too far south) or have not yet been covered in the survey.
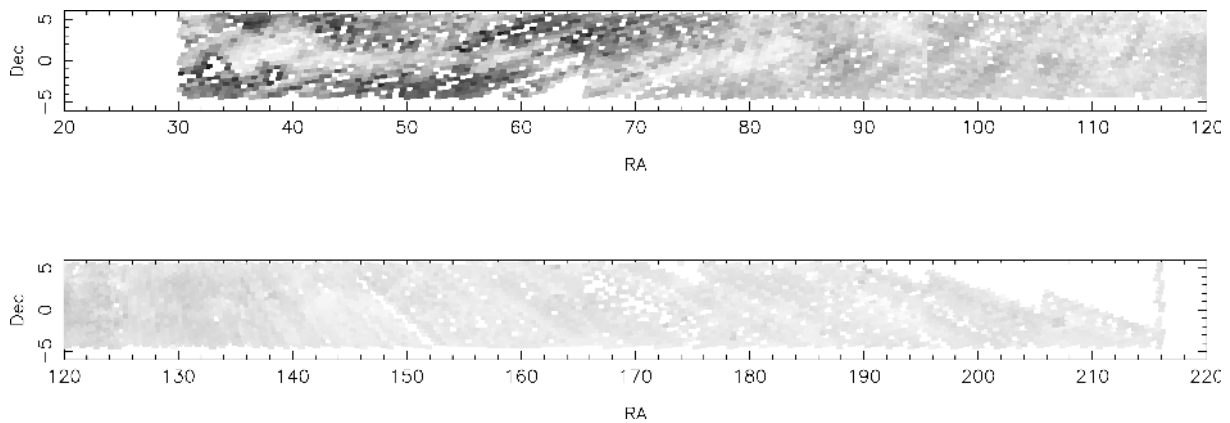

Figure 5. The density of stellar sources in the IPHAS survey with black being most dense and white being less dense. The larger stellar density closer to the Galactic Centre along with the patches of extinction close to the plane in this region can be clearly seen.
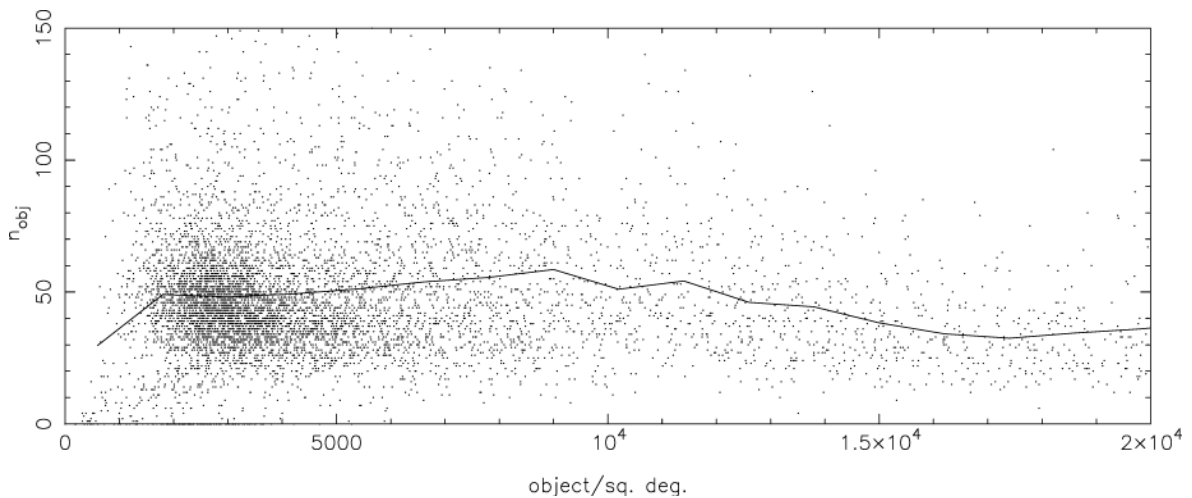

Figure 6. The density of stellar sources in the IPHAS survey for each field versus the number of proper motion objects detected in each field. The solid line shows the mean number of objects for fields binned by stellar density. Note the general trend, dense fields have fewer detected objects. This is because the crowding confusion reduction algorithm removes more of the area of crowded fields.

this main sequence. There is also a white dwarf locus present lying below and to the left of the main sequence. Many objects lie above and to the left of the main sequence. While this may suggest Hα emission, it may also be due to poor photometry in a particular field.

Hence, rather than select all these as potential Hα emitters, in the next section we will use the study of Witham et al. (2008) to identify objects which appear to have significant Hα emission relative to the main sequence on the particular field. Finally, we checked
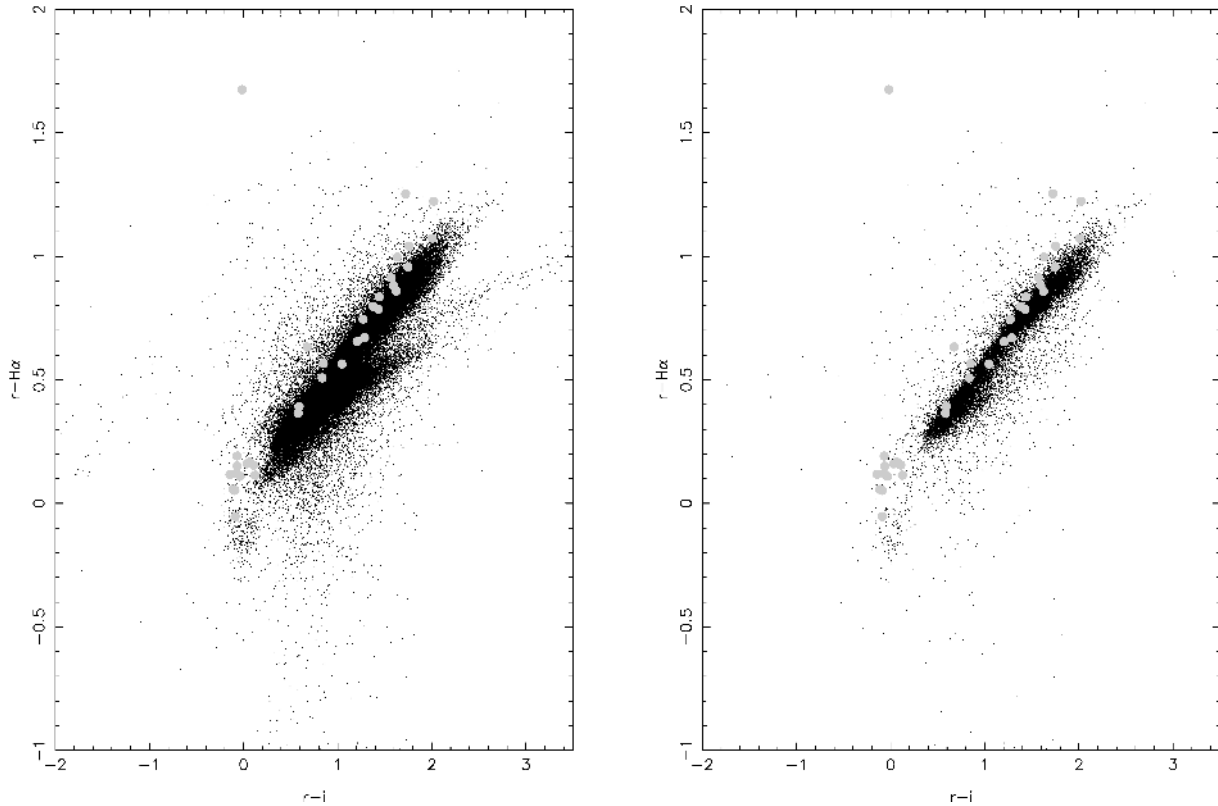
Figure 7. Colour–colour diagrams for the objects. The panel on the left (a) shows all the objects in our sample while the panel on the right (b) shows only those with proper motions greater than 50 mas yr^{-1}. The main stellar locus runs from (0.0,0.1) to (2.0,1.0), this is a near-perfect unreddened main sequence (see Drew et al. 2005). Below and to the left lie the bluer white dwarfs and above and to the left lie potential H$_\alpha$ emitters. The large grey dots represent the objects common between this catalogue and the catalogue of H$_\alpha$ emitters from Witham et al. (2008). These are all plotted on both panels, regardless of their proper motions.

our sample for common proper motion binaries. To investigate if we had a distinct population of common proper motion binaries, we plotted a histogram of the separations of all the objects with proper motions within 2σ of each other. The trend for coincidence objects should be $N \propto r$ and any excess above this at small separations would indicate a separate population of physically bound common proper motion objects. Fig. 8 shows our histogram, clearly there is no distinct population of common proper motion binaries present.

3.1 Comparisons with other IPHAS studies

As stated earlier, the IPHAS survey is currently being exploited for many different scientific goals. One study utilizing IPHAS photometry is that of Witham et al. (2008). Here, IPHAS photometry is used to identify objects which lie significantly above the main stellar locus on a colour–colour diagram similar to Fig. 7. As there will be offsets in the photometry from field to field, Witham et al. (2008) identifies potential Hα emitters relative to the colour–colour diagram for the field the object lies in. Hence, objects which appear to be Hα emitters due to the poor photometry of an individual field are not included in Witham et al's sample. This allows us to treat this data set as a clean sample of potential Hα emitters. Cross-referencing this with our own proper motion sample will remove highly reddened (and distant) Be stars from the Witham sample and should leave only potential Cataclysmic Variables candidates, dMe stars and non-DA white dwarfs (i.e. nearby stellar sources showing either H_α emission or less than expected H_α absorption). In this cross-referencing, we also included objects found in our study with
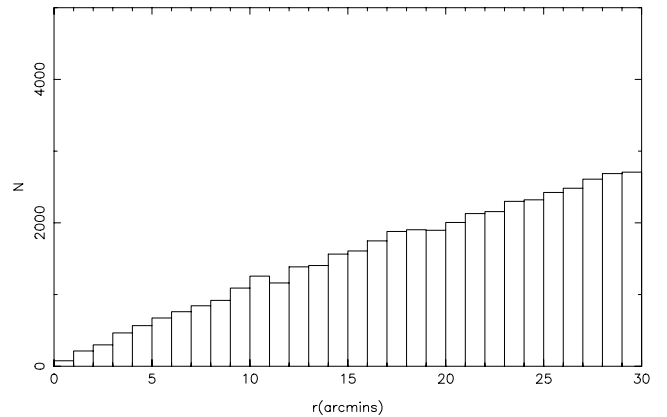

Figure 8. A histogram of the separations of common proper motion pairs in our sample. The trend for coincidence objects would be $N \propto r$. As we see no deviation from this trend at small separations, we conclude that there is no significant population of true common proper motion binaries in our sample.

proper motions between 0.2 and 0.15 arcsec yr^{-1} and objects with r magnitudes between 19 and 20. These were not included in the final catalogue as these objects were found to suffer from a high level of contamination.

The 36 cross-matches are shown in Table 1. Note that eight cross-matches were excluded from this list, and from Figs 3 and 7 after

Table 1. Objects common between our catalogue and the H$_\alpha$ catalogue of Witham et al. (2008).

Name	Position	μ_α (arcsec yr^{-1})	μ_δ (arcsec yr^{-1})	σ_{μ_α} (arcsec yr^{-1})	σ_{μ_δ} (arcsec yr^{-1})	r	i	H$_\alpha$	SpT
IPHASJ000528+663951	00 05 28.05 +66 39 51.5	0.031	−0.051	0.009	0.009[2]	13.582	13.001	13.190	
IPHASJ002156+630635	00 21 56.62 +63 06 35.8	−0.044	−0.026	0.005	0.005[2]	17.105	17.183	16.993	
IPHASJ010749+582709	01 07 49.39 +58 27 09.3	0.022	−0.031	0.005	0.006[2]	14.171	13.279	13.657	
IPHASJ031119+600110	03 11 19.21 +60 01 10.8	0.044	−0.053	0.005	0.006[1]	18.181	15.995	17.058	
IPHASJ032327+534705	03 23 27.39 +53 47 05.4	0.061	−0.054	0.005	0.005[1]	16.734	16.980	16.576	
IPHASJ032825+580645	03 28 25.12 +58 06 45.8	0.144	−0.042	0.006	0.007[2]	17.684	17.917	17.550	
IPHASJ032905+563606	03 29 05.01 +56 36 06.8	−0.019	−0.034	0.006	0.007[2]	14.704	13.503	14.053	
IPHASJ033805+563518	03 38 05.68 +56 35 18.7	0.029	−0.038	0.006	0.006[2]	13.743	12.461	13.077	dMe[2]
IPHASJ034042+573053	03 40 42.96 +57 30 53.7	0.069	−0.033	0.006	0.006[2]	13.724	12.685	13.164	dM[2]
IPHASJ040147+540650	04 01 47.07 +54 06 50.8	0.044	−0.058	0.006	0.007[2]	16.122	14.727	15.361	
IPHASJ043839+410931	04 38 39.38 +41 09 31.9	−0.011	−0.110	0.005	0.006[2]	14.673	14.816	14.556	DB[3]
IPHASJ045400+470031	04 54 00.68 +47 00 31.0	0.004	−0.023	0.006	0.003[1]	17.723	17.691	17.563	
IPHASJ053015+251137	05 30 15.51 +25 11 37.3	0.031	0.044	0.005	0.005[2]	13.429	12.580	12.862	dM[2]
IPHASJ055551+324150	05 55 51.14 +32 41 50.3	−0.037	−0.001	0.006	0.006[2]	17.829	17.707	17.599	DC[2]
IPHASJ055752+274641	05 57 52.90 +27 46 41.8	0.025	−0.044	0.005	0.006[1]	17.264	17.415	17.189	DC[2]
IPHASJ061409+171136	06 14 09.36 +17 11 36.0	0.003	−0.044	0.006	0.006[2]	16.670	14.917	15.628	
IPHASJ062809+163158	06 28 09.40 +16 31 58.7	−0.046	−0.012	0.006	0.006[2]	17.833	17.909	17.642	DB[1]
IPHASJ183523+014245	18 35 23.26 +01 42 45.4	0.154	0.015	0.006	0.006[2]	17.700	16.172	16.921	
IPHASJ184306+004111	18 43 06.88 +00 41 11.3	−0.031	−0.048	0.005	0.005[2]	18.020	18.071	17.930	
IPHASJ185929−040304	18 59 29.38-04 03 04.3	0.051	−0.027	0.005	0.005[2]	13.335	11.604	12.384	
IPHASJ190132+145807	19 01 32.77 +14 58 07.6	0.082	0.076	0.006	0.007[1]	15.905	15.870	15.823	DC[2]
IPHASJ190142−043621	19 01 42.09 −04 36 21.1	0.001	−0.034	0.007	0.006[1]	15.999	14.622	15.201	
IPHASJ190338−025232	19 03 38.54 −02 52 32.4	0.032	−0.010	0.005	0.005[1]	16.514	15.243	15.768	
IPHASJ191733+031937	19 17 33.35 +03 19 37.9	0.138	−0.032	0.005	0.006[2]	15.406	14.984	14.830	
IPHASJ192206+053238	19 22 06.11 +05 32 38.5	0.031	0.000	0.005	0.005[2]	16.254	14.723	15.450	
IPHASJ201409+265254	20 14 09.92 +26 52 54.1	0.035	0.038	0.005	0.006[1]	15.113	13.408	14.187	
IPHASJ210541+534334	21 05 41.78 +53 43 34.5	0.025	−0.020	0.005	0.005[2]	14.891	13.451	14.055	
IPHASJ210923+515607	21 09 23.85 +51 56 07.8	0.027	0.038	0.006	0.006[2]	17.632	15.631	16.531	
IPHASJ210951+425705	21 09 51.24 +42 57 05.1	0.192	−0.018	0.010	0.005[1]	15.552	15.559	15.340	DB[4]
IPHASJ215029+554250	21 50 29.23 +55 42 50.6	0.027	0.006	0.005	0.005[1]	17.477	15.492	16.283	
IPHASJ223541+590745	22 35 41.31 +59 07 45.7	0.026	−0.005	0.004	0.005[1]	16.644	16.729	16.547	
IPHASJ224918+614903	22 49 18.57 +61 49 03.9	−0.039	−0.023	0.004	0.005[2]	17.508	17.475	17.436	DA[1]
IPHASJ225040+632838	22 50 40.03 +63 28 38.2	0.102	−0.037	0.005	0.006[2]	16.389	16.406	14.714	CV[5]
IPHASJ232003+571736	23 20 03.28 +57 17 36.6	−0.035	0.000	0.007	0.007[2]	13.537	12.965	13.170	
IPHASJ232158+581034	23 21 58.03 +58 10 34.6	0.030	−0.011	0.006	0.005[1]	16.037	14.454	15.129	
IPHASJ232908+615911	23 29 08.78 +61 59 11.0	−0.183	−0.067	0.007	0.004[2]	17.626	17.304	17.330	DC[1]

Note. IPHASJ225040+632838 is the known proper motion CV system GD 552 (Greenstein & Giclas 1978), IPHASJ043839+410931 is GD 61 (Giclas et al. 1965), IPHASJ210951+425705 is EGGR 334 (Greenstein 1974) and IPHASJ032825+580645 is the known high proper motion star LSPM J0328+5806 (Lepine & Shara 2005). Spectral type sources: [1]WHT spectroscopy; [2]FAST spectroscopy; [3]Giclas et al. 1965; [4]Greenstein (1974); [5]Greenstein & Giclas 1978.

inspection of the images by eye found that they may be blended together with unrelated background objects on the POSS-I plates. Examining Fig. 7 we can see that many of the grey dots (representing Witham et al.'s Hα emitters with significant proper motions) fall along the main sequence. It is possible that these are true Hα emitters and appear in this part of the diagram due to uncorrected field-to-field photometric offsets or some selection effect. Of these objects, one (IPHASJ053015+251137) appears to share a common proper motion with the nearby (separation 42 arcsec) star TYC 1852-777-1 (Hog et al. 1998). The two proper motions agree within 1σ implying these are a true bound pair or part of the same moving group. Three other objects redder than $r - i = 0.4$ have spectra from Fase Spectrograph for the Tillinghast Telescope (FAST) followup observations of IPHAS sources. Of these, one (IPHASJ033805+563518) was found to be an M dwarf with Hα emission. The question remains as to why these objects appeared in Witham et al.'s catalogue. Witham et al. fitted a curve to the unreddened main sequence in each field and identified emitters as objects which lay significantly above this curve. The two non-emitting M dwarfs lie in the brightest selection bin of Witham et al.'s selection process ($r < 16$). Here, the number

of objects defining the unreddened main sequence will be smallest. It could be that these are marginal selections where the unreddened main sequence is affected by poor statistics. It is also possible that these are objects with variable weak Hα emission. One moderately red object (IPHASJ191733+031937) appears to lie on the subdwarf sequence.

15 of the cross-matches objects which appear to lie on the white dwarf sequence in the reduced proper motion diagram (Fig. 3). Of these, IPHASJ225040+632838 is the low-state CV system GD 552 (Greenstein & Giclas 1978). Another two, IPHASJ043839+410931 (GD 61; Giclas, Burnham & Thomas 1965) and IPHASJ210951+425705 (EGGR 334; Greenstein 1974), are known DB white dwarfs. Additionally, three objects had spectra taken in the IPHAS spectroscopic followup programme with the FAST spectrograph on the 1.5-m Tillinghast telescope on Mount Hopkins. Of the remaining nine objects, three had spectra taken using the Intermediate dispersion Spectroscopic and Imaging System spectrograph on the William Herschel Telescope (WHT) on La Palma. These spectra were used to provide rough spectral classifications which can be found in Table 1. Seven of the eight spectrally
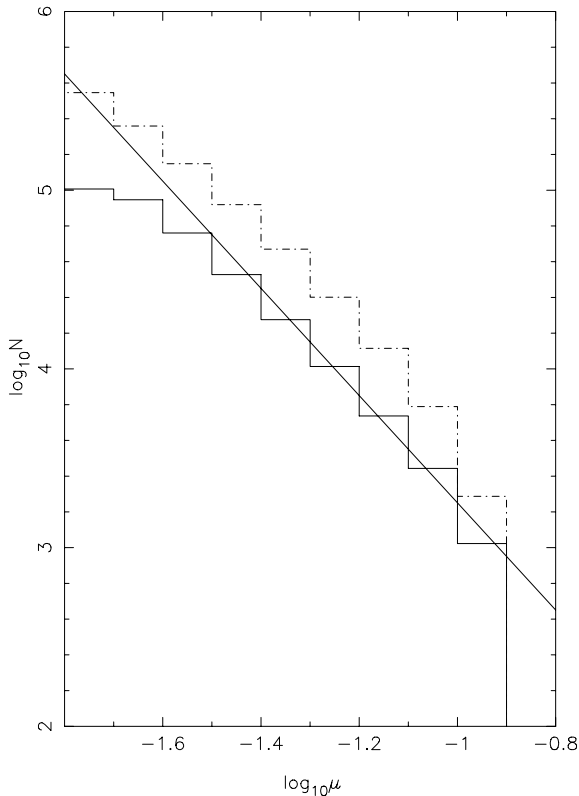
Figure 9. A cumulative proper motion histogram for our the objects in our catalogue. The solid line represents the $N \propto \mu^{-3}$ relation that would be expected with no incompleteness. It is clear that our survey begins to become incomplete below about 60 mas yr^{-1} and that below 20 mas yr^{-1} there are virtually no objects. The dotted line represents the study of Gould & Kollmeier (2004). Clearly, their study is complete to lower proper motions than ours. In the region where our survey is most complete, there is a factor of 2 difference between the numbers.

classified objects which lie bluewards of $r - i = 0.4$ in the colour–colour diagram (excluding the known CV GD 552) are non-DA white dwarfs. Hence, we believe the remaining objects are good non-DA white dwarf candidates.

Valdivielso et al. (2009) have produced a sample of young, low-mass objects using IPHAS data. Clearly identifying the proper motions of such objects could establish a connection with a known star-forming association or moving group. Unfortunately, none of these objects appear in our catalogue.

4 DISCUSSION

In order to provide a rough estimate of our completeness, we plotted a cumulative proper motion histogram. This is shown in Fig. 9. Assuming uniform spatial and velocity distributions and a fully complete survey, the distribution should scale as $N \propto \mu^{-3}$. This is represented by the solid line in the plot. It is clear that we begin to become incomplete below 60 mas yr^{-1}. This is due to a combination of our limiting magnitude and some objects falling in fields with poor astrometry (hence having proper motions which are not significant enough). Below about 25 mas yr^{-1}, it is clear the distribution flattens off and we can say we have no significant population below this mark. We have also compared our results with those in Gould & Kollmeier (2004). Fig. 9 shows that in the proper motion range where both surveys have similar proper motion completeness we have half of the number of objects that Gould & Kollmeier have.

This is despite the two surveys having similar areas (both around 1400 deg^2). However, our survey covers a much more crowded area than theirs. Deacon, Hambly & Cooke (2005) calculated the area lost to bright and blended stars across the southern sky. Examining their Fig. 10, it is clear that in the southern regions of the sky at similar Galactic latitude to ours the completeness is often 50 per cent or worse. Hence, we believe this difference in numbers is due the more crowded nature of our survey area.

The IPHAS survey consists of 15 270 pointings, which between them cover the 1800 deg^2 survey area twice or more. Hence, simply taking the size of the detector and multiplying it by the number of fields our survey covers (12 362) will not yield an accurate estimate of our current survey area. A rough estimate can be provided by multiplying the fraction of the fields we cover (approximately 81 per cent) by the total final survey area of 1800 deg^2. This yields and approximate area for our proper motion survey of 1457 deg^2. However, as stated above, due to crowding we are only likely to identify proper motion objects in roughly half of this total area. Once data from the few unobserved IPHAS fields have been released, we will apply the same method to the remaining fields, completing our proper motion survey.

In calculating our astrometric solutions, we use sets of reference stars. These may have small bulk motions. Additionally, for the objects where we have too few reference stars the raw IPHAS positions are used. These are tied to the 2MASS (Skrutskie et al. 2006) system using reference stars. Hence, we will measure proper motions relative to these reference stars rather than absolute proper motions. Lepine (2008) also encountered this problem. They concluded that the difference between absolute and relative proper motions was typically less than their measurement errors. As our measurement errors are similar to theirs (typically below their quoted global errors of 8 mas yr^{-1} in each axis), we deduce that any offset between the relative and absolute proper motions of our sample will also be below our calculated errors.

5 CONCLUSIONS

We have completed the first comprehensive wide-field proper motion survey of the northern Galactic plane ($|b| < 5°$) covering proper motions between 150 and approximately 30 arcsec yr^{-1}. This sample covers a large section (1457 deg^2) of the northern plane and contains 57 249 objects with significant proper motions. We also identify 17 objects in common between our catalogue and the Hα emission catalogue of Witham et al. (2008). These objects fell in to two distinct groups, a blue group dominated by non-DA white dwarfs and a red group dominated by marginally selected ordinary main-sequence objects. This sample will clearly be useful in the study of populations such as white dwarfs and subdwarfs in the Galactic plane. We will seek to complete the catalogue for the full survey area and use the upcoming UVEX data to extend it to higher proper motions above the current imposed limit of 0.15 arcsec yr^{-1}.

REFERENCES

Deacon N. R., Hambly N. C., 2007, A&A, 468, 163
Deacon N. R., Hambly N. C., Cooke J. A., 2005, A&A, 435, 363
Drew J. E. et al., 2005, MNRAS, 362, 753
Fedorov P. N., Myznikov A. A., Akhmetov V. S., 2009, MNRAS, 393, 133
Finch C. T., Henry T. J., Subasavage J. P., Jao W. C., Hambly N. C., 2007, AJ, 133, 2898
Folkes S. L., Pinfield D. J., Kendall T. R., Jones H. R. A., 2007, MNRAS, 378, 901
Giclas H. L., Burnham R., Thomas N. G., 1965, Lowell Obs. Bull., 6, 155
Gonzalez-Solares E. A. et al., 2008, MNRAS, 388, 89
Gould A., Kollmeier J. A., 2004, ApJS, 152, 103
Greenstein J. L., 1974, ApJ, 189, 131
Greenstein J. L., Giclas H., 1978, PASP, 90, 460
Groot P. J., 2009, MNRAS, in press (arXiv:0906.3498)
Hambly N. C. et al., 2001, MNRAS, 326, 1279
Hog E., Kuzmin A., Bastian U., Fabricius C., Kuimov K., Lindegren L., Makarov V. V., Roeser S., 1998, A&A, 335, 65
Lawrence A. et al., 2007, MNRAS, 379, 1599
Lepine S., 2008, AJ, 135, 2177
Lepine S., Shara M. M., 2005, AJ, 129, 3, 1483
Lucas P. W. et al., 2008, MNRAS, 391, 136
Luyten W. J., 1922, Lick Observatory Bulletin, 10, 135
Luyten W. J., 1979a, Luyten Half Arcsecond Catalogue. University of Minnesota, Minneaplois
Luyten W. J., 1979b, New Luyten Two Tenths Catalogue, University of Minnesota, Minneapolis
Mampaso A. et al., 2006, A&A, 458, 203
Pokorny R. S., Jones H. R. A., Hambly N. C., Pinfield D. J., 2003, A&A, 397, 575
Sale S. E., Drew J. E., Unruh Y. C., 2009, MNRAS, 392, 497
Skrutskie M. F. et al., 2006, AJ, 131, 1163
Valdivielso L. et al., 2009, A&A, 497, 973
Vink J. S., Drew J. E., Steeghs D., Wright N. J., Martin E. L., Gänsicke B. T., Greimel R., Drake J., 2008, MNRAS, 387, 308
Wallace P. T., 1998, Starlink User Note No., 67.42: SLALIB: Postitional Astronomy Library, CCLRC/Rutherford Appleton Laboratory, PPARC
Wesson R. et al., 2008, ApJ, 688, L21
Witham A. R., Knigge C., Drew J. E., Greimel R., Steeghs D., Gänsicke B. T., Groot P. J., Mampaso A., 2008, MNRAS, 384, 1277

APPENDIX A: EXAMPLE OF DATA TABLE

The data tables for this paper will be available in the online version (see Supporting Information). Here we give an example of one of the data tables.

Table A1. An example of the data tables available electronically for this paper.

Name	Position J2000	μ_α (arcsec yr^{-1})	μ_δ (arcsec yr^{-1})	σ_{μ_α} (arcsec yr^{-1})	σ_{μ_δ} (arcsec yr^{-1})	r	i	Hα	MJD
IPHASJ000001+575210	00 00 01.48 +57 52 10.9	−0.009	−0.034	0.008	0.004[2]	15.278	14.700	14.956	53666
IPHASJ000001+652057	00 00 01.81 +65 20 57.0	0.002	−0.029	0.007	0.005[2]	14.995	14.214	14.627	53664
IPHASJ000005+644818	00 00 05.67 +64 48 18.2	−0.001	−0.044	0.006	0.005[2]	18.923	17.575	18.455	53664
IPHASJ000005+602518	00 00 05.81 +60 25 18.0	0.036	0.010	0.005	0.005[1]	17.328	16.598	16.927	53665
IPHASJ000009+652017	00 00 09.09 +65 20 17.2	−0.078	0.008	0.007	0.006[2]	19.885	18.113	19.235	53664
IPHASJ000010+602519	00 00 10.07 +60 25 19.7	−0.059	−0.025	0.009	0.007[2]	13.659	12.837	13.184	53666
IPHASJ000013+582109	00 00 13.26 +58 21 09.5	−0.032	−0.029	0.007	0.004[2]	17.388	15.783	16.565	53665
IPHASJ000014+631007	00 00 14.91 +63 10 07.1	0.035	−0.004	0.006	0.006[1]	16.513	15.365	15.879	53666
IPHASJ000017+664726	00 00 17.51 +66 47 26.4	−0.023	−0.05	0.006	0.006[2]	12.748	12.328	12.519	54009
IPHASJ000017+620139	00 00 17.51 +62 01 39.0	0.037	−0.001	0.007	0.008[1]	17.660	15.958	16.761	53244
IPHASJ000018+592623	00 00 18.76 +59 26 23.4	0.072	−0.027	0.004	0.007[1]	16.140	14.542	15.308	53666
IPHASJ000023+661414	00 00 23.88 +66 14 14.3	0.038	0.005	0.005	0.007[1]	17.770	16.107	16.977	53666

Note. [1] indicates astrometric solutions calculated from reference stars, [2] implies the astrometric errors are drawn from global error estimates. The Modified Julian date (MJD) and the position are both taken from the IPHAS observations.

SUPPORTING INFORMATION

Additional Supporting Information may be found in the online version of this article.

APPENDIX A. DATA TABLES.

Please note: Wiley-Blackwell are not responsible for the content or functionality of any supporting materials supplied by the authors. Any queries (other than missing material) should be directed to the corresponding author for the article.

This paper has been typeset from a TEX/LATEX file prepared by the author.